Structural Information on the ECR Plasma by X-ray Imaging

ECRIS2016
The 22nd International Workshop on ECR Ion Sources

R. Rácz, S. Biri, J. Pálinkás

Institute for Nuclear Research
Hungarian Academy of Sciences (Atomki)
Debrecen, Hungary

D. Mascali, G. Castro, C. Caliri, L. Neri, F. P. Romano, S. Gammino

Instituto Nazionale di Fisica Nucleare
Laboratori Nazionali del Sud
Catania, Italy

Outline

- Introduction
- Experimental setup
- Plasma images
  - Exposing methods
  - Spectrally integrated images
    - Frequency dependence
    - Power dependence
    - Axial magnetic field dependence
  - Spectrally resolved images
    - Spectral information
    - Spectral information in ROIs
    - Spectral filtering
    - Plasma distribution vs frequency

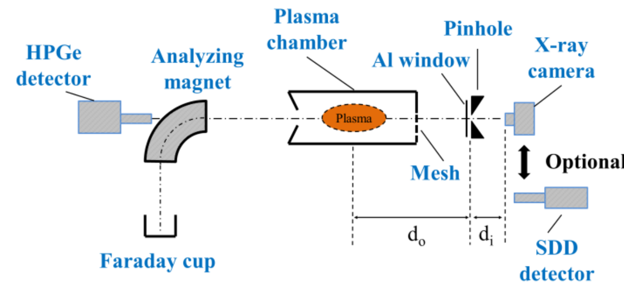

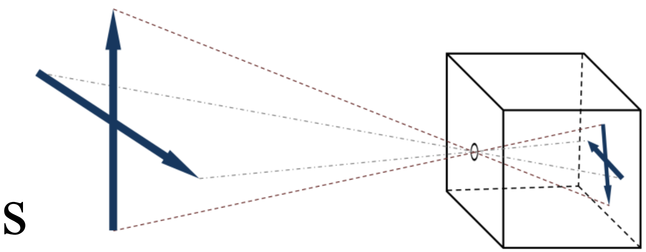

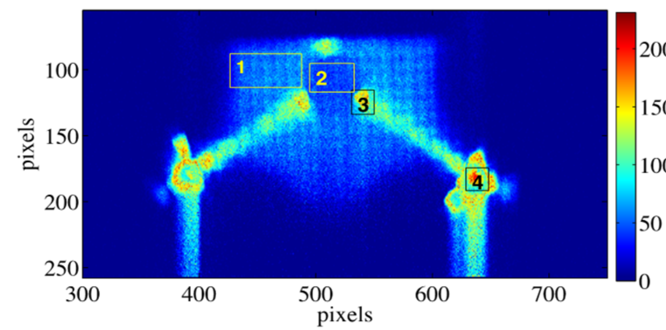

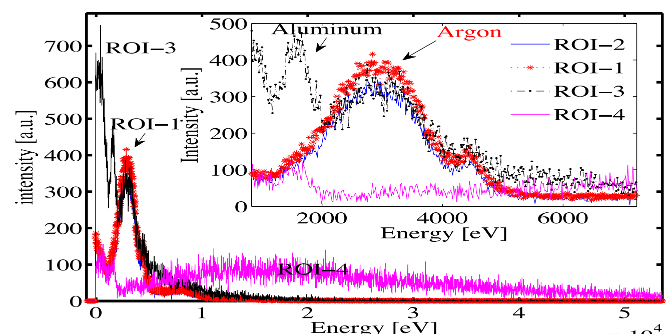

Why to know the ECR plasma (fine) structure?

- Plasma structure → extracted ion beam parameters (emittance brightness)

L. Celona et al. RSI 2008

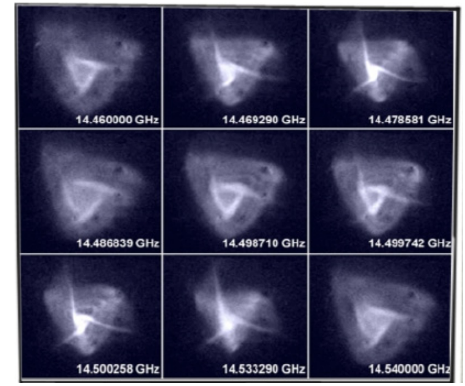

- Density profile →
  - To explain the plasma instabilities
  - For implementation of alternative heating methods (e.g. modal conversion)

O. Tarvainen et al. PSST 2014

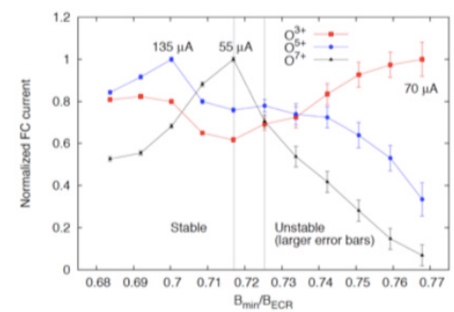

- To improve the general microwave-to-plasma coupling efficiency

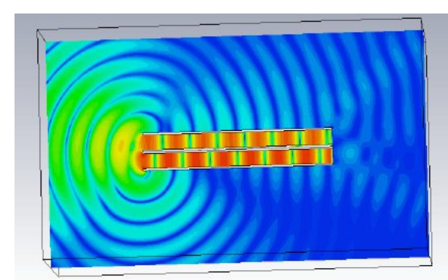

How to know the ECR plasma (fine) structure?

- Invasive method: Langmuir-probe

ENSAR2/MIDAS training

Cylindrical Langmuir- probe

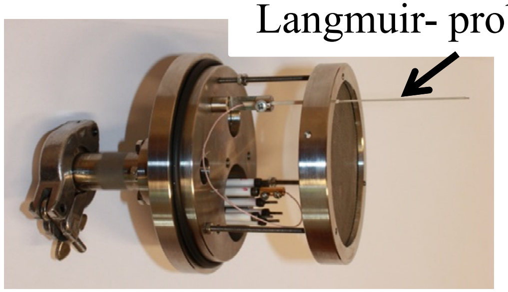

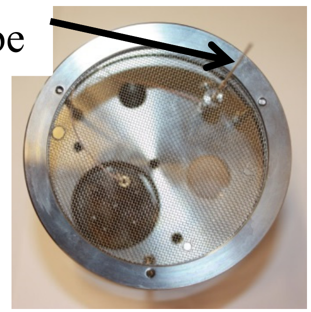

I-V curve

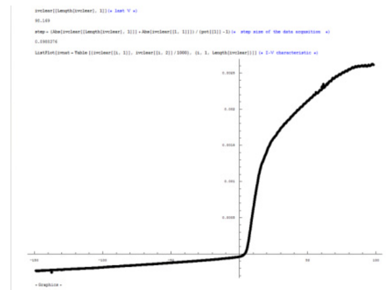

Local plasma parameters:
- Density
- Temperature
- Plasma potential
- EEDF

- Noninvasive method: emission profile by imaging

Visible light

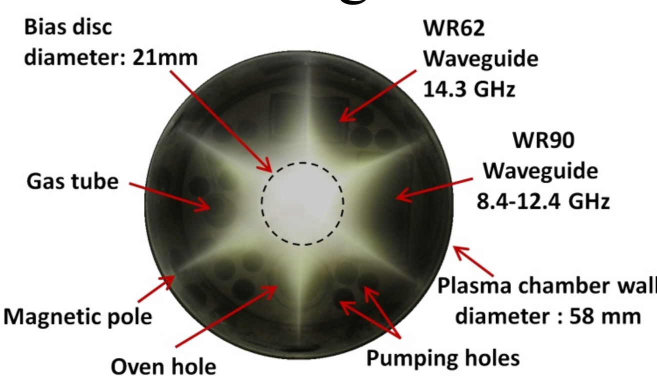

R. Rácz, ECRIS16, Busan, Korea, 29 August 2016

Information on

Cold electrons

Warm electrons

X-ray

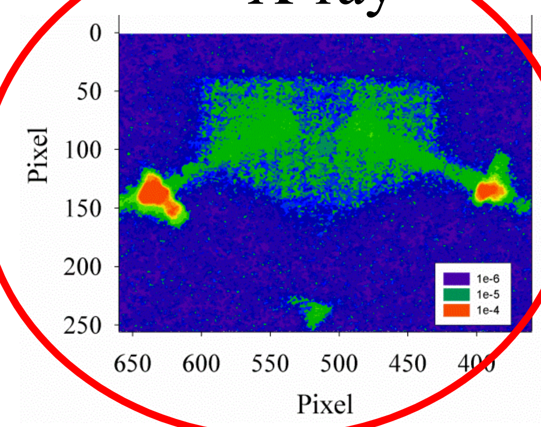

Using pinhole X-ray camera (camera obscura)

Object

Pinhole Image

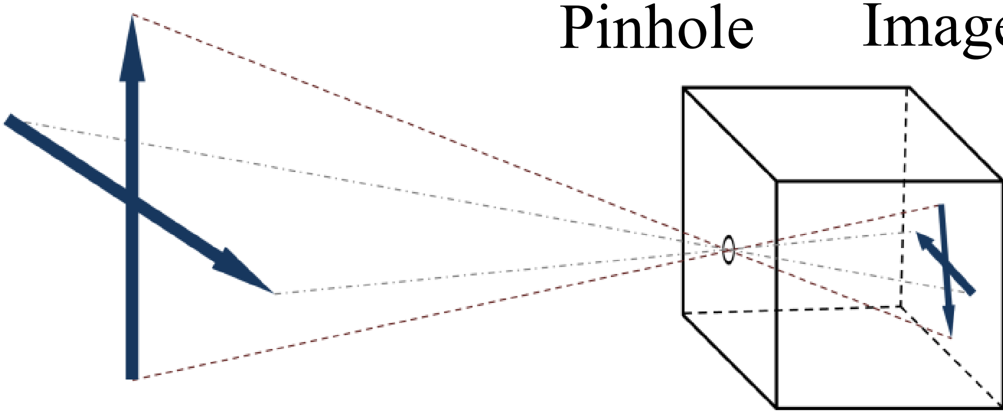

- For visible light imaging used from the 11th century
- The 'simplest' method for imaging
- No lens
- Infinite depth of field
- Perspective view
- The best way for X-ray imaging

X-ray

Plasma

~ 100 um pinhole

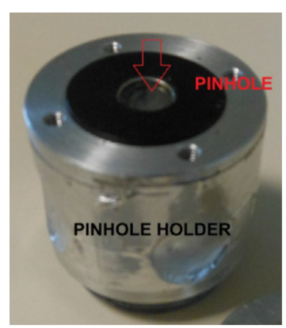

X-ray CCD

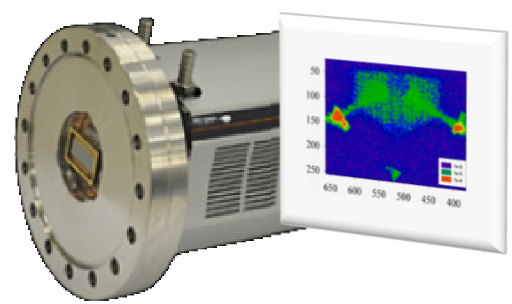

Background

- X-ray CCD and pin-hole camera are widely used in the stellar X-ray astronomy.

- For ECR plasma imaging the pioneer was the Atomki ECR Group (2002/2003)
  - To develop the technique for ECR plasmas
  - To get general information on the structural changes as function of some ECR setting parameters

- New efforts in 2014 by Atomki and INFN-LNS groups: wider instrumentation, more focused aims

Max Plank Institute
Orion in
Visible light X-ray

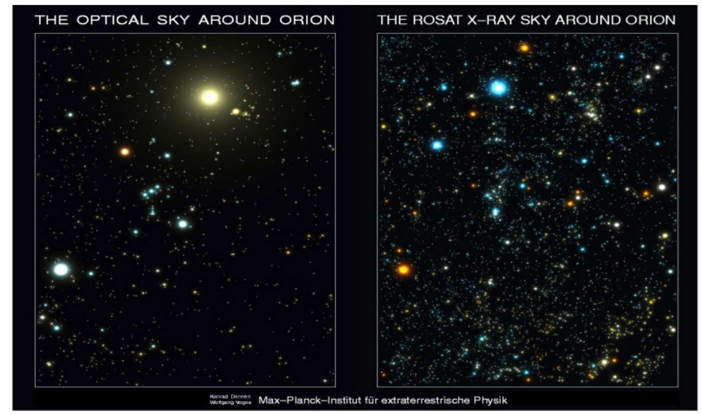

Atomki ECR group
ECR plasma in
Visible light X-ray

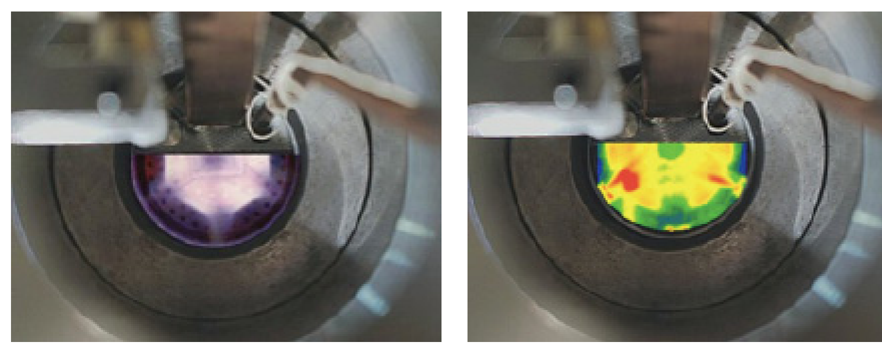

S. Biri et al. RSI 2004

Background – 2014 Experiment

Results of volumetric measurements and preliminary results

ICIS 2015

REVIEW OF SCIENTIFIC INSTRUMENTS **87**, 02A510 (2016)

Electron cyclotron resonance ion source plasma characterization by X-ray spectroscopy and X-ray imaging

David Mascali,[1,a)] Giuseppe Castro,[1] Sándor Biri,[2] Richárd Rácz,[2] József Pálinkás,[2] Claudia Caliri,[1,3] Luigi Celona,[1] Lorenzo Neri,[1] Francesco Paolo Romano,[1,4] Giuseppe Torrisi,[1,5] and Santo Gammino[1]

[1]*INFN–Laboratori Nazionali del Sud, Via S. Sofia 62, 95125 Catania, Italy*
[2]*Institute for Nuclear Research (Atomki), Hungarian Academy of Sciences, Bem tér 18/c, H-4026 Debrecen, Hungary*
[3]*Università degli Studi di Catania, Dip.to di Fisica e Astronomia, via Santa Sofia 64, 95123 Catania, Italy*
[4]*CNR, Istituto per i Beni Archeologici e Monumentali, Via Biblioteca 4, 95124 Catania, Italy*
[5]*Università Mediterranea di Reggio Calabria, DIIES, Via Graziella, I-89100 Reggio Calabria, Italy*

(Presented 26 August 2015; received 20 August 2015; accepted 9 December 2015; published online 6 January 2016)

An experimental campaign aiming to investigate electron cyclotron resonance (ECR) plasma X-ray emission has been recently carried out at the ECRISs—Electron Cyclotron Resonance Ion Sources laboratory of Atomki based on a collaboration between the Debrecen and Catania ECR teams. In a first series, the X-ray spectroscopy was performed through silicon drift detectors and high purity

REVIEW OF SCIENTIFIC INSTRUMENTS **87**, 02A741 (2016)

X-ray pinhole camera setups used in the Atomki ECR Laboratory for plasma diagnostics

R. Rácz,[1,a)] S. Biri,[1] J. Pálinkás,[1] D. Mascali,[2] G. Castro,[2] C. Caliri,[2] F. P. Romano,[2,3] and S. Gammino[2]

[1]*Institute for Nuclear Research (Atomki), Hungarian Academy of Sciences, Bem tér 18/C, H-4026 Debrecen, Hungary*
[2]*Instituto Nazionale di Fisica Nucleare—Laboratori Nazionali del Sud, via S. Sofia 62, 95123 Catania, Italy*
[3]*CNR, Istituto per i Beni Archeologici e Monumentali, Via Biblioteca 4, 95124 Catania, Italy*

(Presented 27 August 2015; received 21 August 2015; accepted 30 September 2015; published online 23 December 2015)

Imaging of the electron cyclotron resonance (ECR) plasmas by using CCD camera in combination with a pinhole is a non-destructive diagnostics method to record the strongly inhomogeneous spatial density distribution of the X-ray emitted by the plasma and by the chamber walls. This method can provide information on the location of the collisions between warm electrons and multiple charged ions/atoms, opening the possibility to investigate the direct effect of the ion source tuning parameters to the plasma structure. The first successful experiment with a pinhole X-ray camera was carried out

Comparison of the former and 2014 setups and preliminary results

ICIS 2015

Outline

- Introduction
- **Experimental setup**
- Plasma images
  - Exposing methods
  - Spectrally integrated images
    - Frequency dependence
    - Power dependence
    - Axial magnetic field dependence
  - Spectrally resolved images
    - Spectral information
    - Spectral information in ROIs
    - Spectral filtering
    - Plasma distribution vs frequency

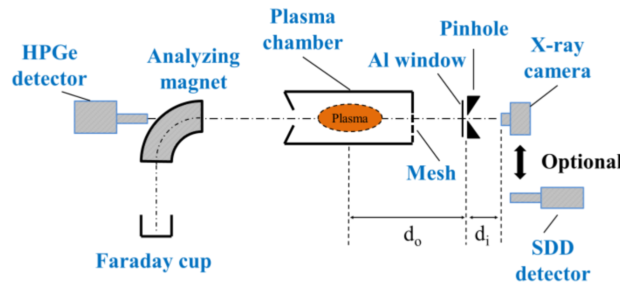

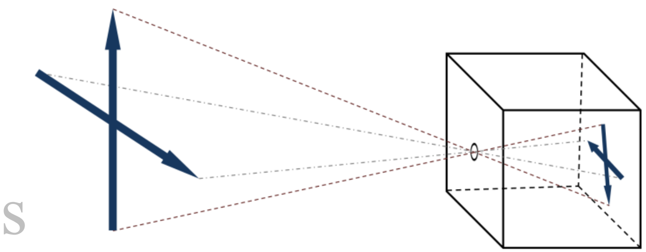

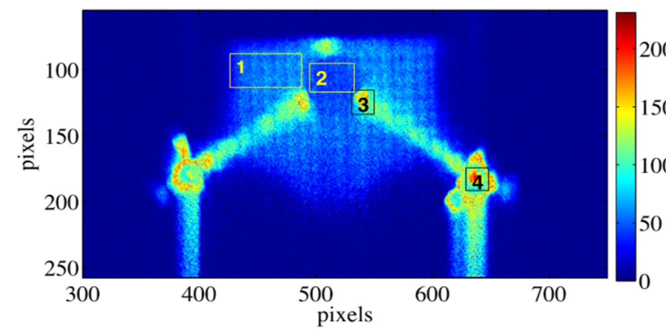

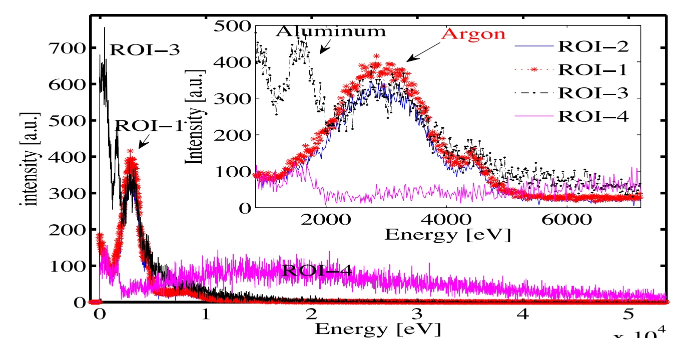

Experimental setup

Atomki ECR laboratory

14.3 GHz ECRIS

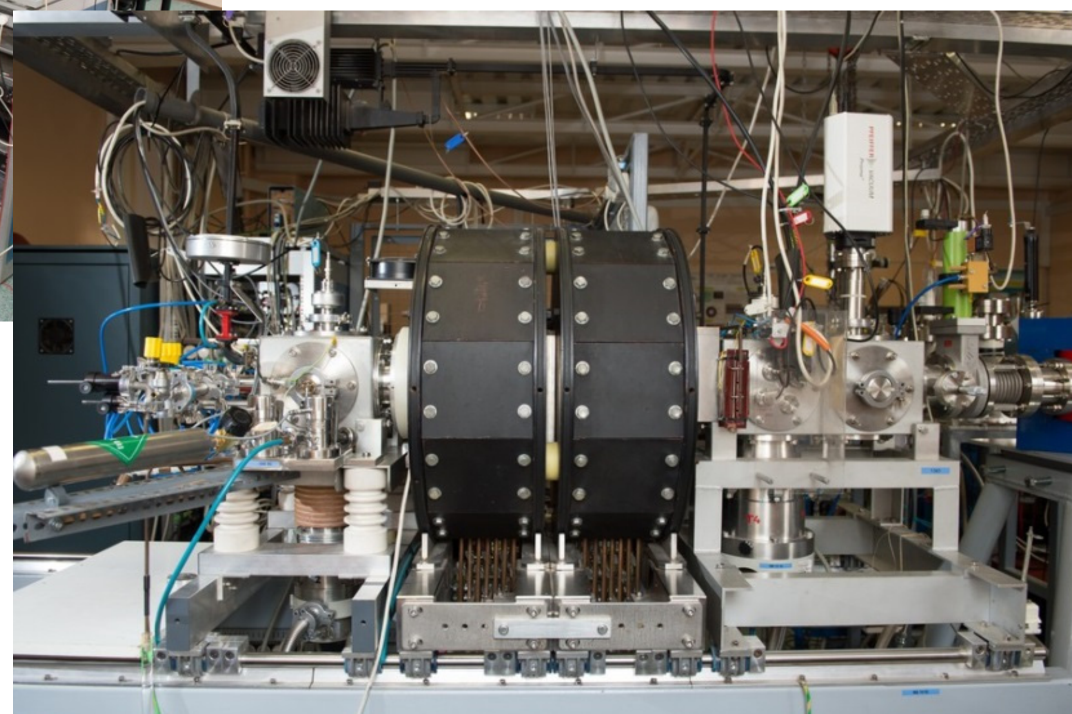

- Permanent magnet hexapole and room temperate coils
- No post acceleration
- Used for atomic physics, material science, ECR plasma physics

Experimental setup

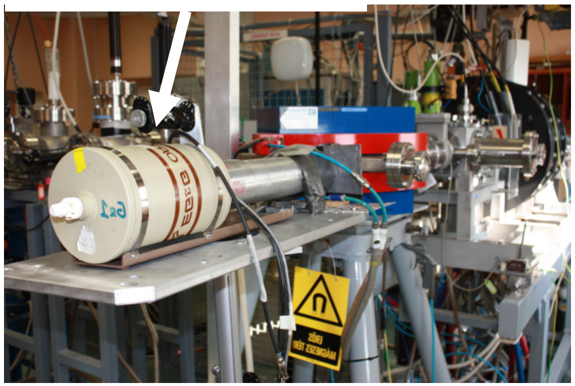

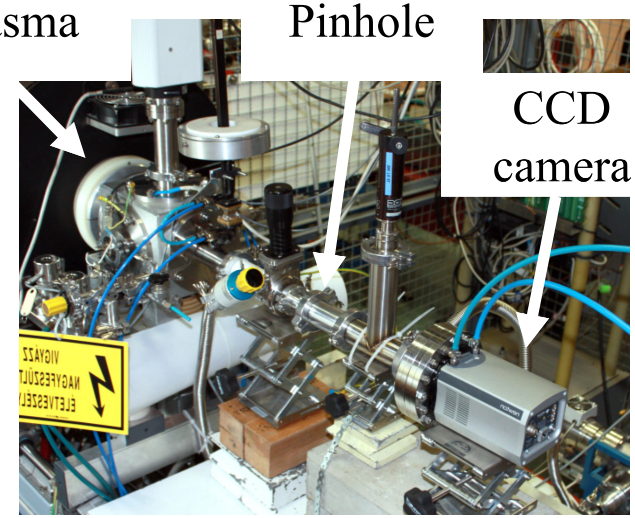

Andor Technology-Newton CCD camera	
Senzor size	27.6 mm x 6.9 mm
Pixels	1024 x 255
Energy resolution	150 eV
Energy range	1 – 10 keV
Magnification	0.082/0.124/0.158
Pinhole	100 um Pb

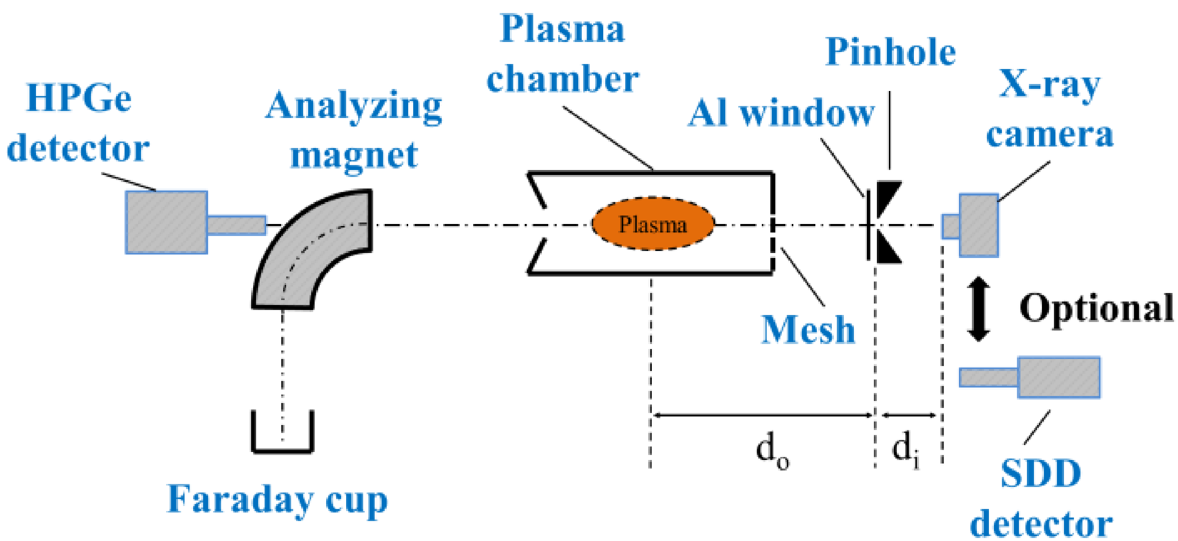

Experimental setup

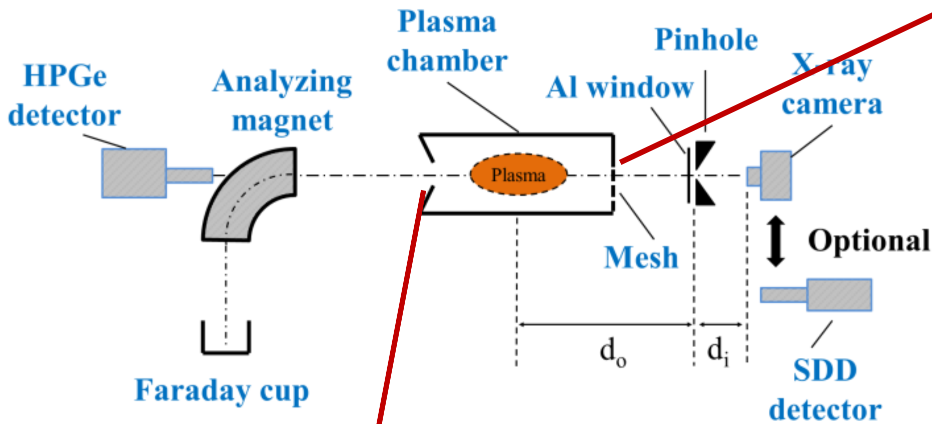

Injection Plate

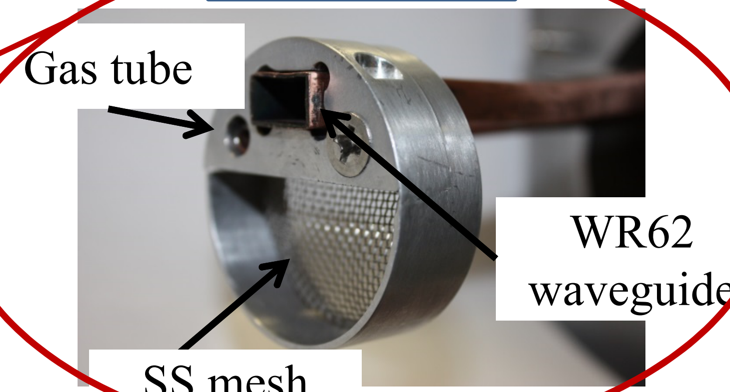

Al - Plasma electrode

Plasma is seen by eye

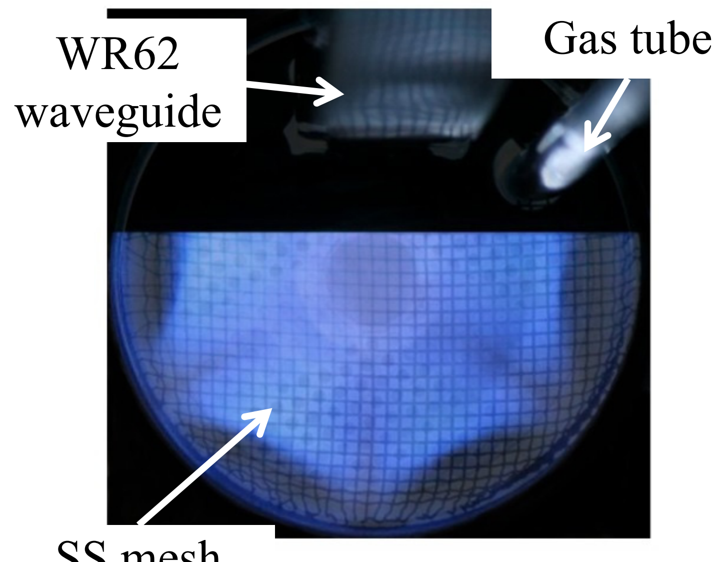

Selection of working points

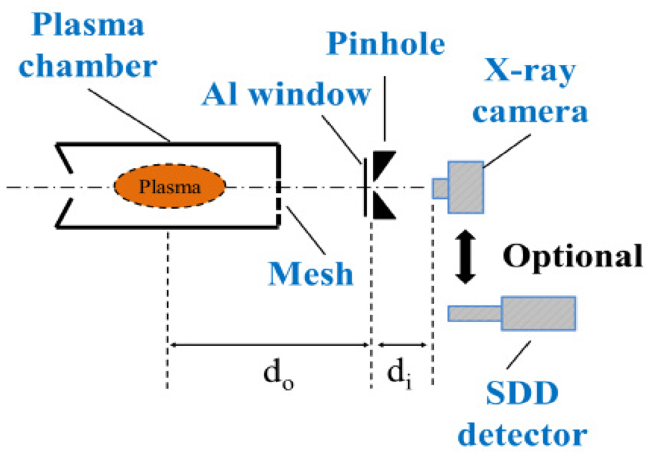

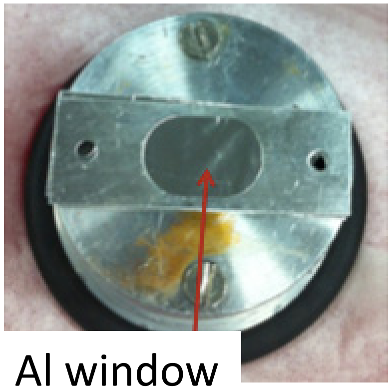

- Magnification (the highest the best) $M = d_i/d_o$
- Thickness of Al window (D_{Al}), optimal: noise (UV, VL) – signal (X-ray) ratio

M/D_{Al}	1 um	3 um	6 um
0.082			(A)
0.124	(B)		
0.158		(C)	

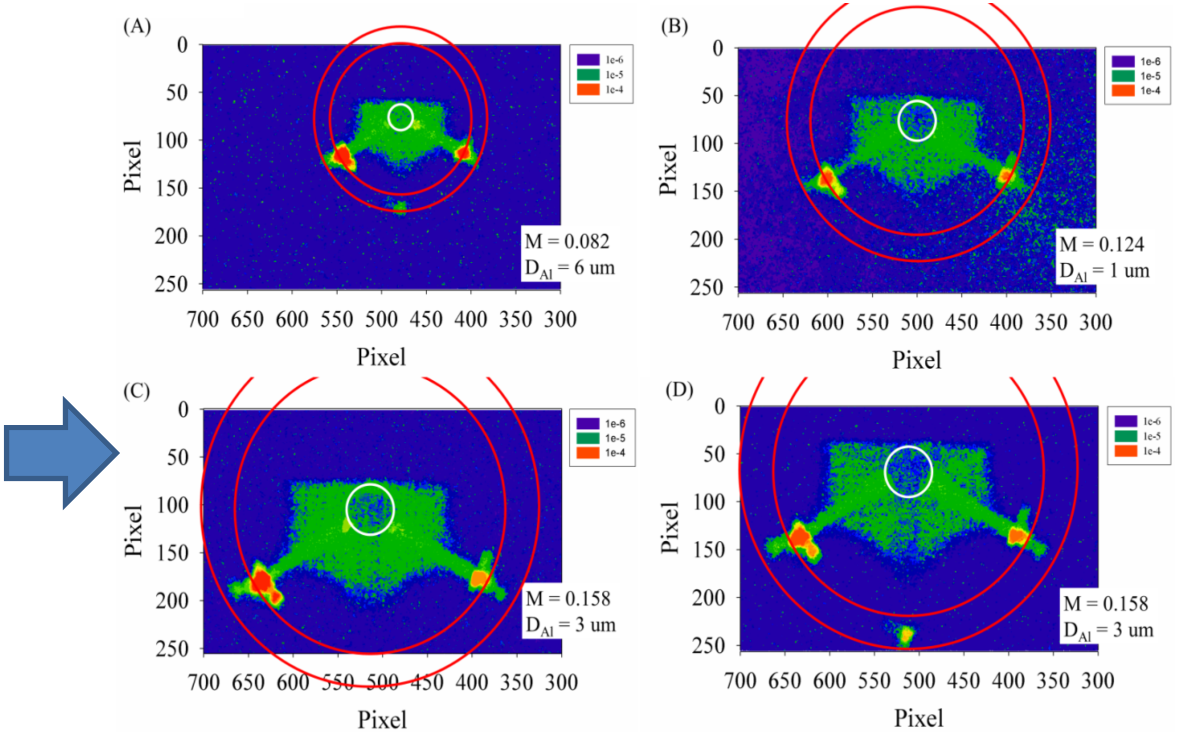

Outline

- Introduction
- Experimental setup
- Plasma images
  - Exposing methods
  - Spectrally integrated images
    - Frequency dependence
    - Power dependence
    - Axial magnetic field dependence
  - Spectrally resolved images
    - Spectral information
    - Spectral information in ROIs
    - Spectral filtering
    - Plasma distribution vs frequency

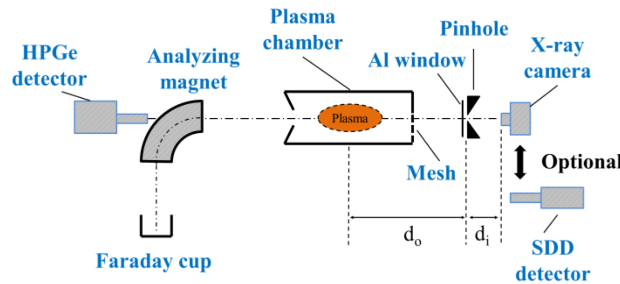

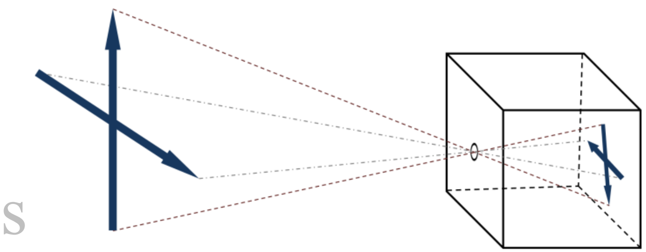

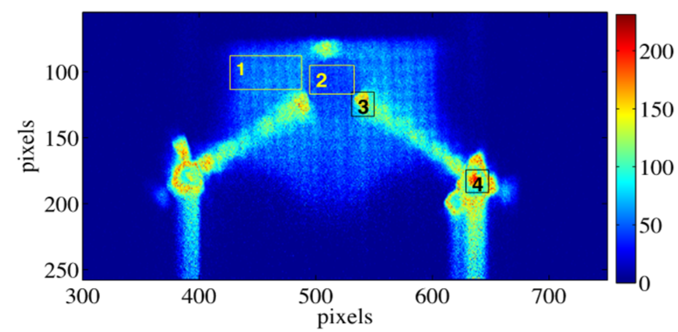

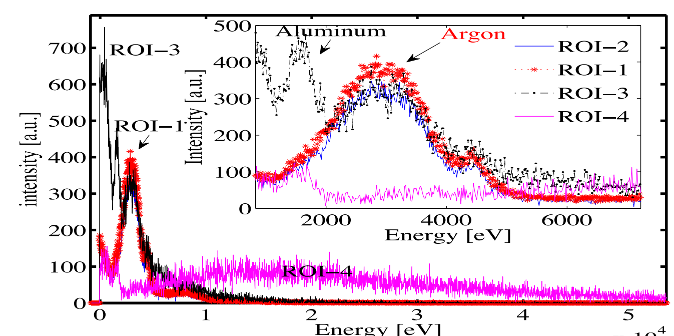

Spectrally integrated images

Acquisition

0	0	0	1	0	0	0	0
1	0	0	0	0	1	0	0
0	1	0	1	0	1	0	0
0	1	0	1	0	0	0	0
0	0	1	1	0	0	0	0
1	0	1	0	0	0	0	0
0	0	0	0	1	0	1	0
0	1	0	0	0	0	0	0

- Long exposure time: several 10 s, to avoid the blooming of the CCD
- One frame for one image
- Individual pixels can be loaded by many X-ray photons → no spectral information
- Spectrally integrated but spatially resolved structural information

Spectrally integrated images

Acquisition

0	0	0	17	0	0	0	0
42	0	0	0	0	73	0	0
0	50	0	40	0	30	0	0
0	72	0	11	0	0	0	0
0	0	56	47	0	0	0	0
17	0	60	0	0	0	0	0
0	0	0	0	43	0	72	0
0	50	0	0	0	0	0	0

- Long exposure time: several 10 s, to avoid the blooming of the CCD
- One frame for one image
- Individual pixels can be loaded by many X-ray photons → no spectral information
- Spectrally integrated but spatially resolved structural information

Photon counting mode

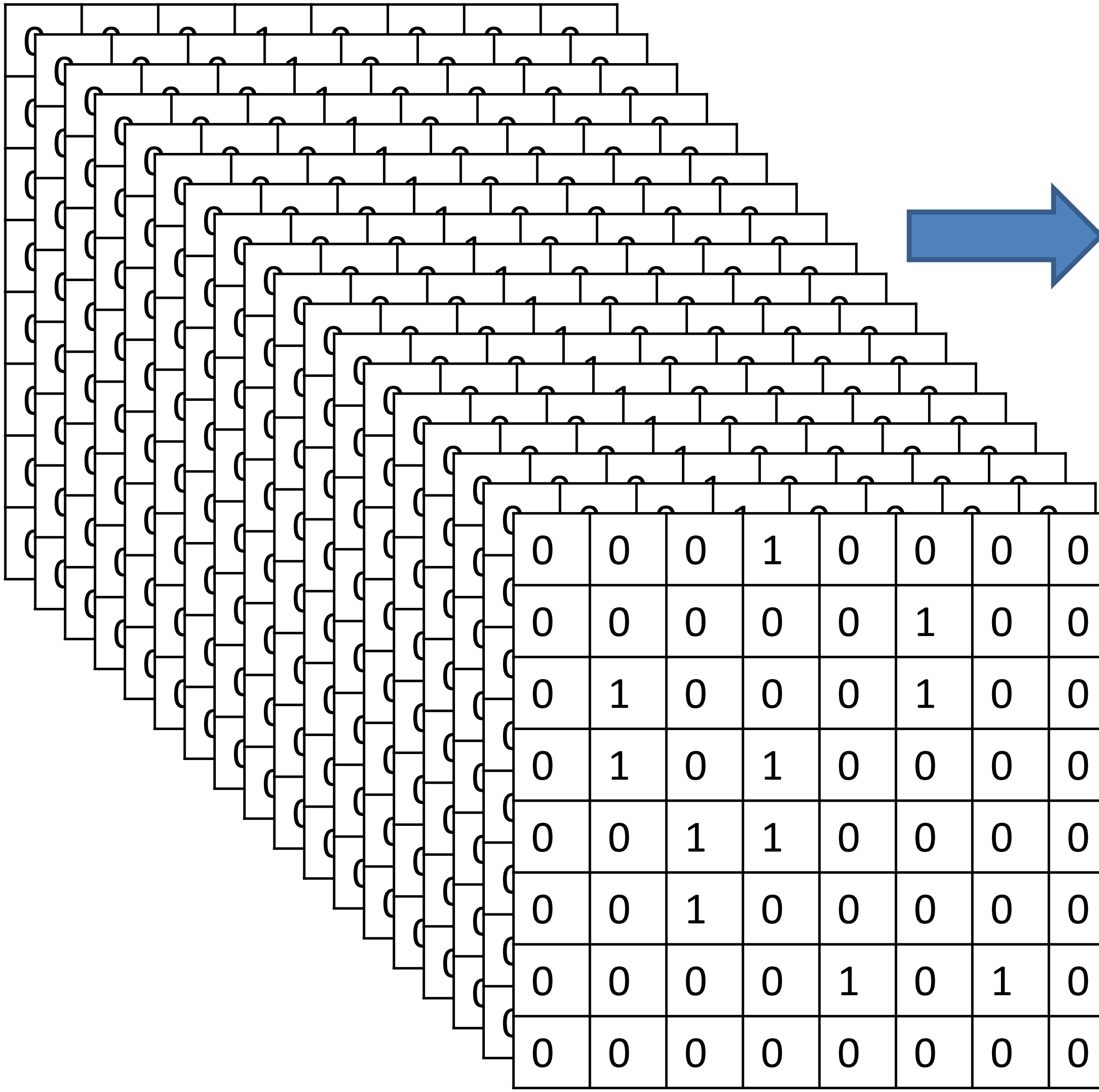

0	0	0	1	0	0	0	0
0	0	0	0	0	1	0	0
0	1	0	0	0	1	0	0
0	1	0	1	0	0	0	0
0	0	1	1	0	0	0	0
0	0	1	0	0	0	0	0
0	0	0	0	1	0	1	0
0	0	0	0	0	0	0	0

0	0	0	17	0	0	0	0
1	0	0	0	0	25	0	0
0	47	0	25	0	1	0	0
0	9	0	1	0	0	0	0
0	0	30	20	0	0	0	0
1	0	1	0	0	0	0	0
0	0	0	0	1	0	1	0
0	1	0	0	0	0	0	0

- Short exposure time (ms)
- Thousands of frames for one image
- Individual pixels as a single photon detector
- Spectrally and spatially resolved information

Outline

- Introduction
- Experimental setup
- Plasma images
  - Exposing methods
  - Spectrally integrated images
    - Frequency dependence
    - Power dependence
    - Axial magnetic field dependence
  - Spectrally resolved images
    - Spectral information
    - Spectral information in ROIs
    - Spectral filtering
    - Plasma distribution vs frequency

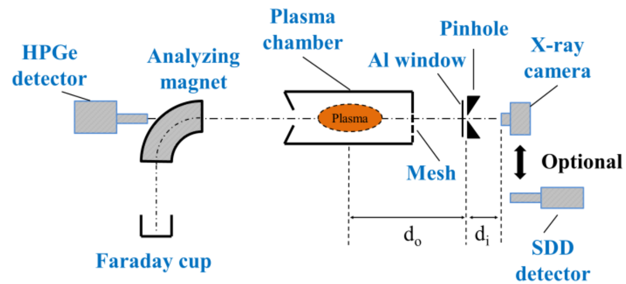

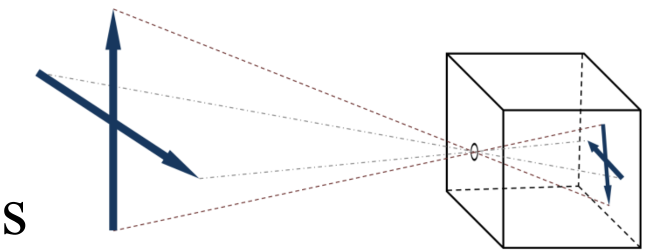

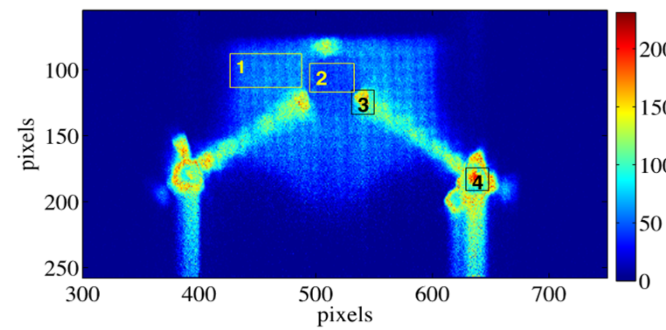

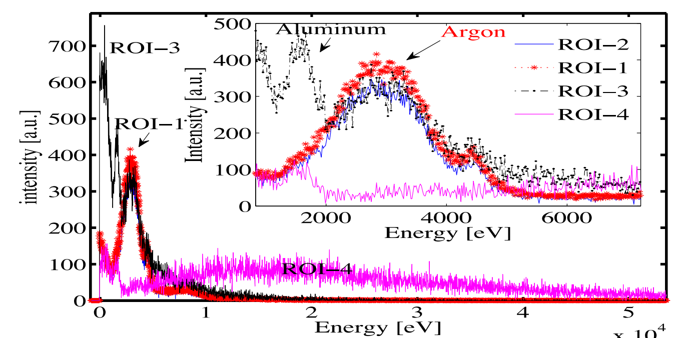

Spectrally integrated images frequency dependence

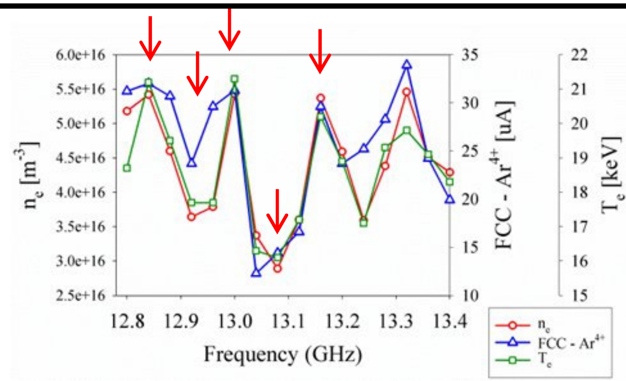

D. Mascali et al. RSI 2015

From volumetric measurements strong correlation between n_e, T_e, <Q>, FCC-Ar^{4+} vs rf frequency

- Frequency: varied between 12.84 GHz and 13.16 GHz with 80 MHz steps
- Microwave power: 30 W
- Gas: Ar
- The strength of the magnetic trap was maximal (100 % coils currents)
- M = 0.082
- D_{Al} = 6 um
- Normalized images

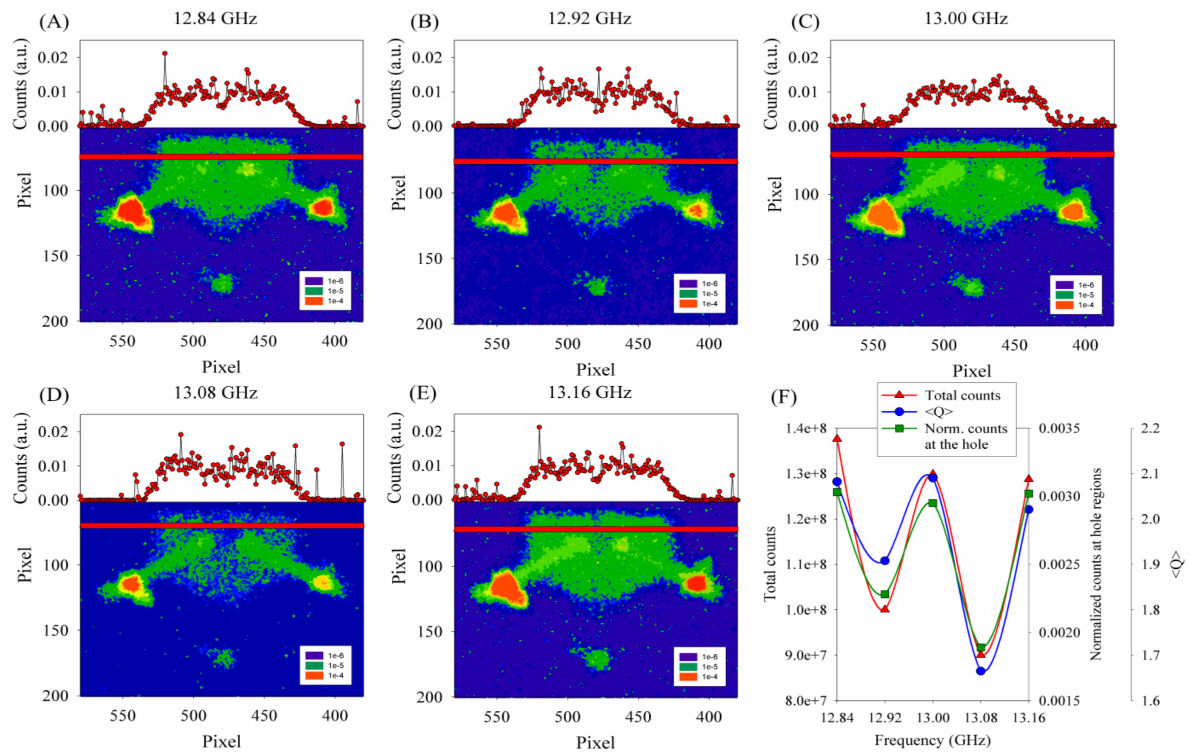

- Strong effect of the rf frequency on the plasma images especially in the near axis region
- The total counts measured at the near axis regions (extraction hole) respect to the total counts of the images are also following the fluctuation pointed by the volumetric measurements → structure vs ionization efficiency

Spectrally integrated images
<u>power dependence</u>

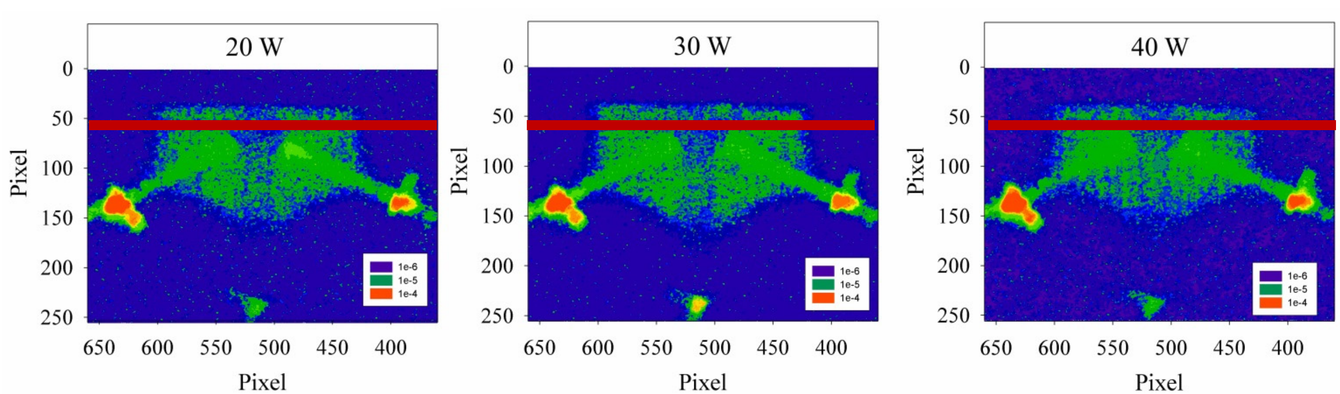

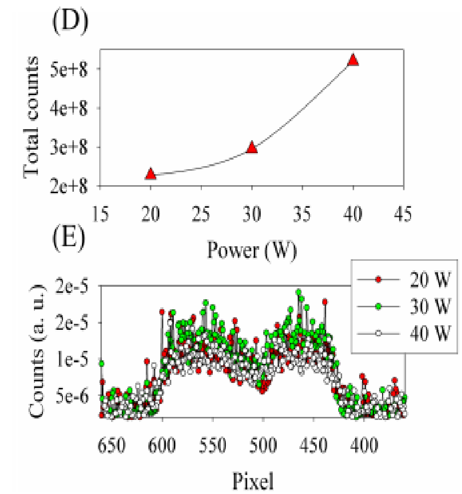

- Microwave power: 20 W – 40 W
- Frequency: 12.84 GHz
- Gas: Ar
- The strength of the magnetic trap was maximal (100 % coils currents)
- M = 0.158
- D_{Al} = 3 um
- t_{exp}= 40 sec
- Normalized images

- Total counts of the images are increasing with the applied power
- No remarkable structural changes as shown by horizontal distribution profiles

Spectrally integrated images
B dependence

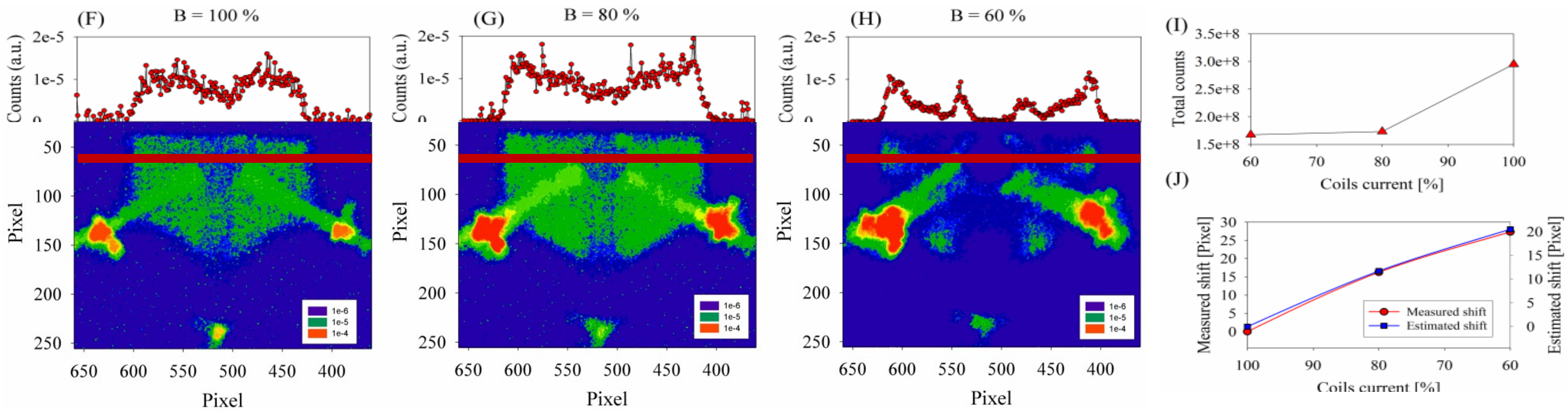

- The strength of the magnetic trap: 100%, 80%, 60% coils currents
- Microwave power: 30W
- Frequency: 12.84 GHz
- Gas: Ar
- M = 0.158
- D_{Al} = 3 um
- t_{exp}= 40 sec
- Normalized images

- Total counts of the images are increasing with the applied coils currents
- Strong effect of the B on the plasma images
- Plasma images in the near axis region becomes emptier at each reduction step (horizontal profiles)
- Plasma is expanding and is shifting toward the plasma chamber wall
- This shift can be explained by the radial expand of the resonant surface

Outline

- Introduction
- Experimental setup
- Plasma images
  - Exposing methods
  - Spectrally integrated images
    - Frequency dependence
    - Power dependence
    - Axial magnetic field dependence
  - **Spectrally resolved images**
    - **Spectral information**
    - **Spectral information in ROIs**
    - **Spectral filtering**
    - **Plasma distribution vs frequency**

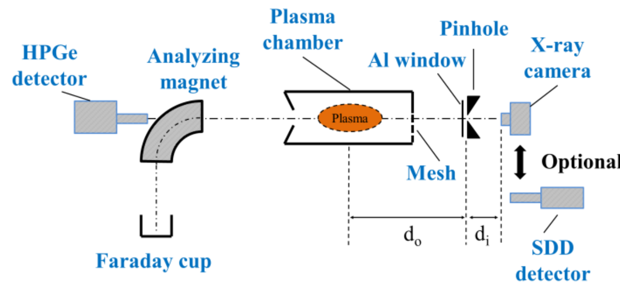

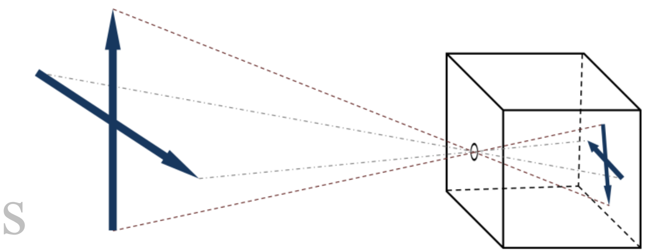

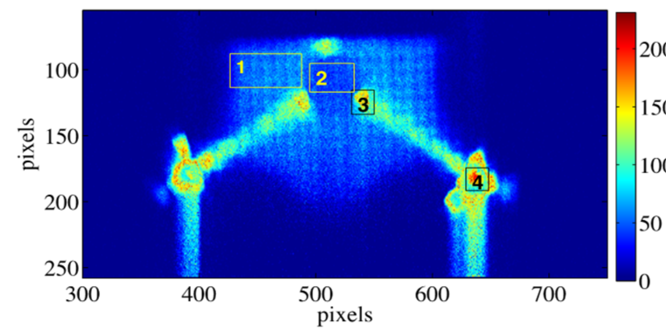

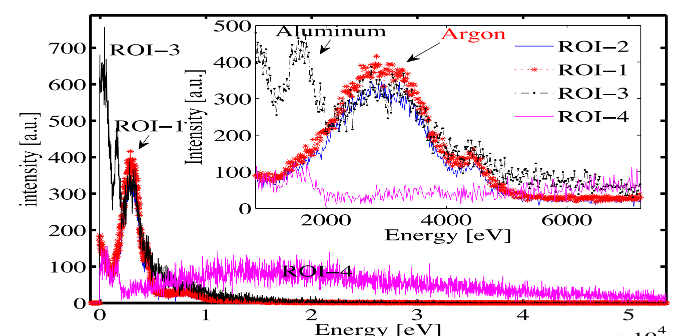

Spectral information

Superposition of the photon counted frames

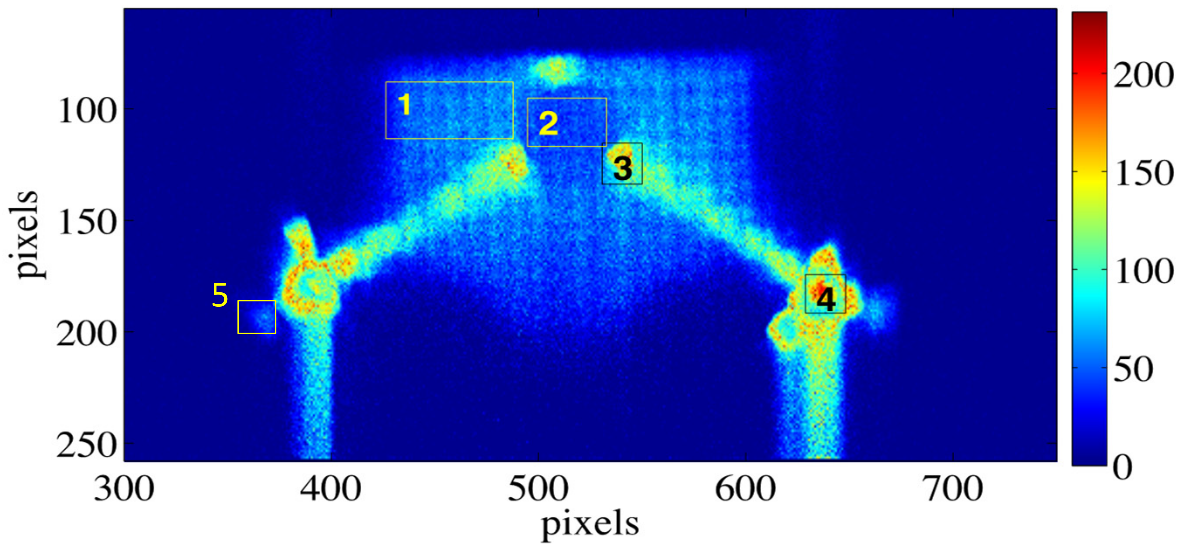

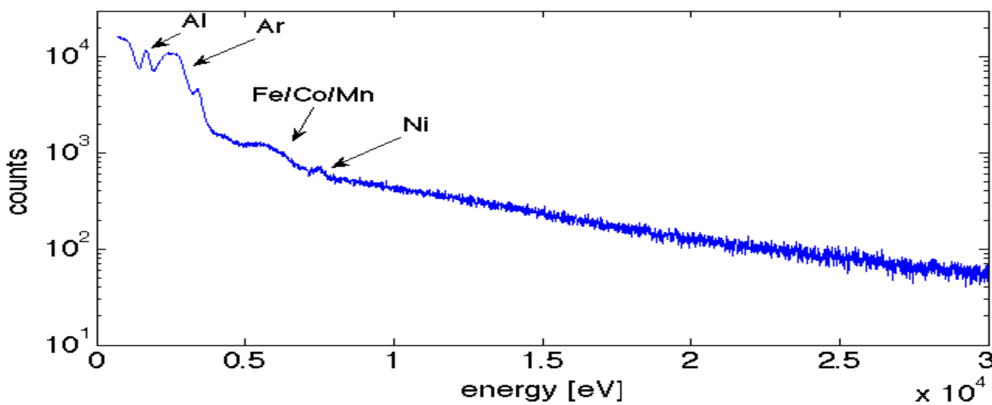

- Number of frames: 3500
- Exposure time of one frame: 150 ms
- Plasma parameters:

100 % coils current, P = 30W, f = 12.84 GHz, Ar plasma

- ROIs: 1)Plasma region 2) extraction hole region, 3) extraction plate, 4) extraction plate, 5)lateral wall of the plasma chamber

Spectra of the whole image

R. Rácz, ECRIS16, Busan, Korea, 29 August 2016

Spectral information in ROIs

Superposition of the photon counted frames

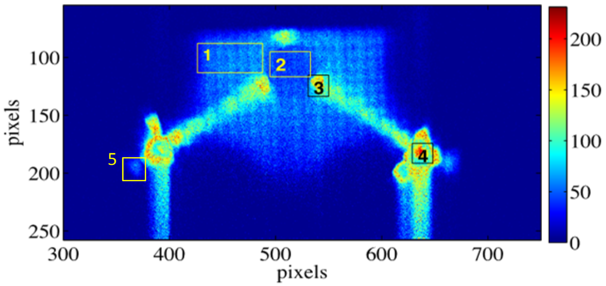

Spectral comparison at different ROIs

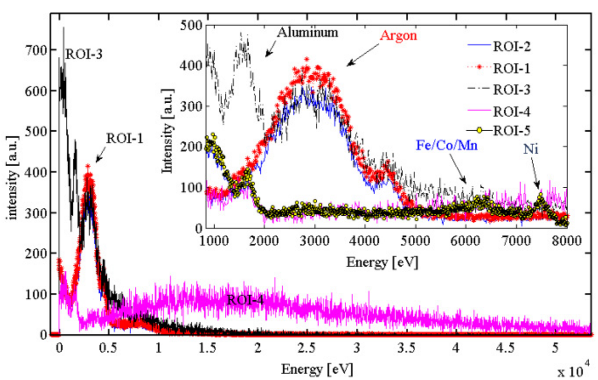

Spectra of the selected ROIs

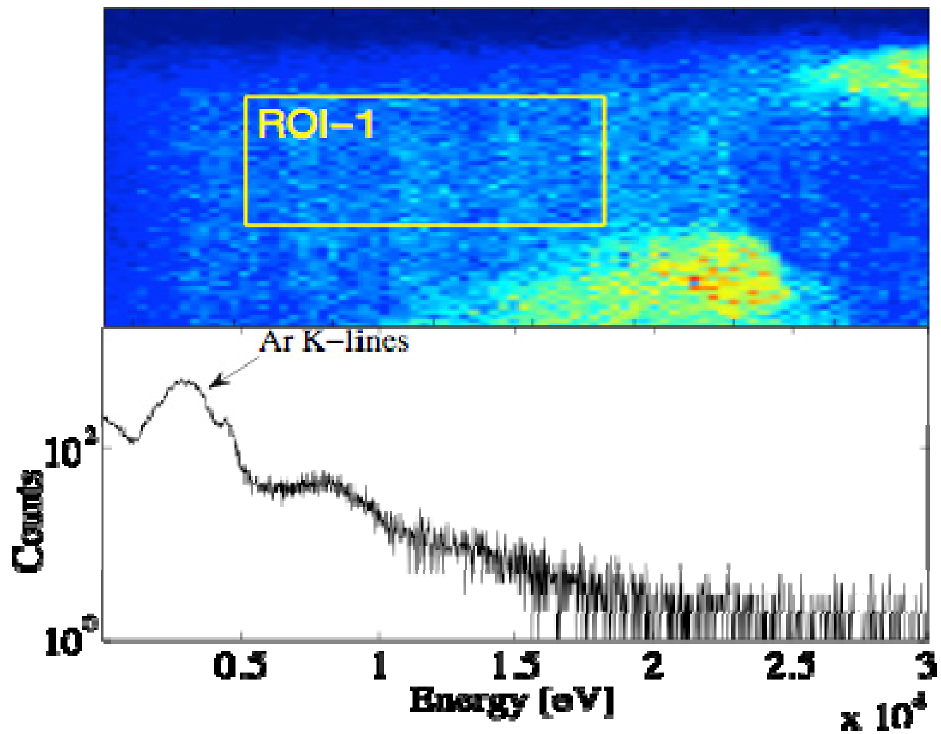

- Intense Argon K peak at ROI-1 and ROI-2 → corresponding to the Ar plasma
- Aluminum K peak at ROI-4 → corresponds to the Al plasma electrode
- ROI-3 shows the characteristics of both groups (ROI-1-2, and ROI-4) → axial inspection
- ROI-5 shows K peaks of Fe/Co/Mn and Ni → lateral wall of the SS plasma chamber

Spectral information in ROIs

Superposition of the photon counted frames

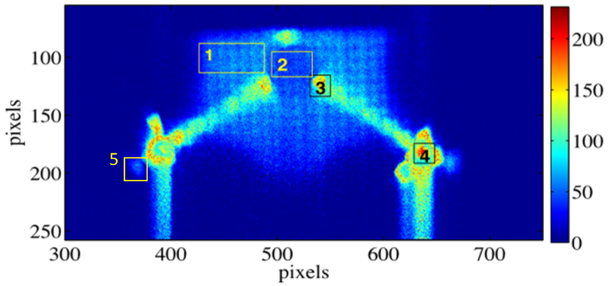

Spectral comparison at different ROIs

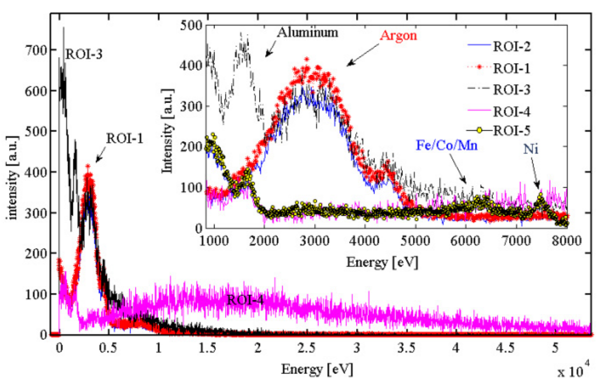

Spectra of the selected ROIs

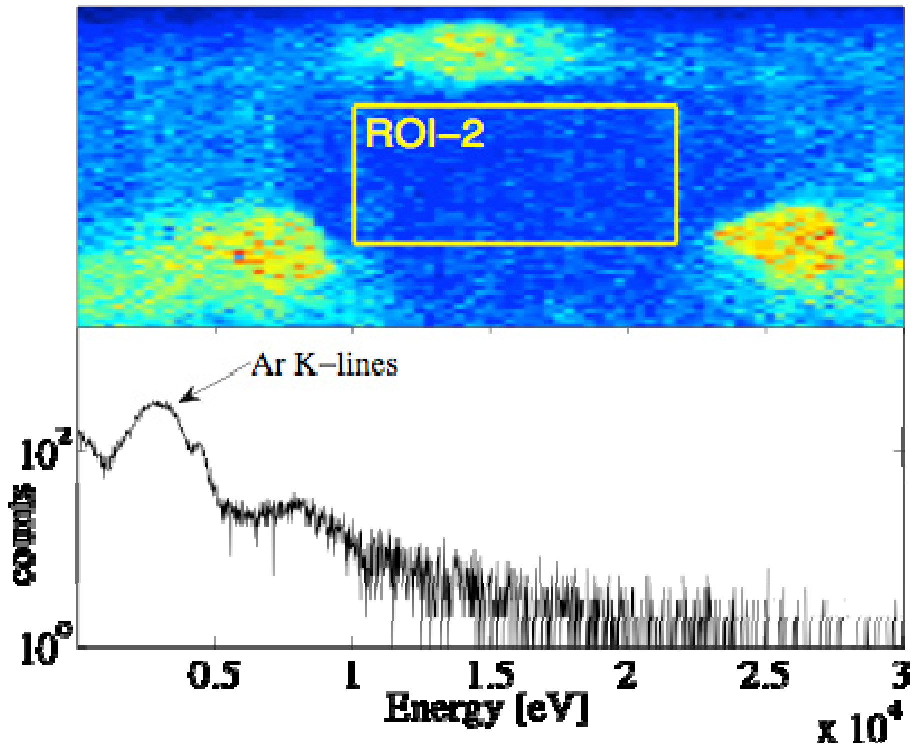

- Intense Argon K peak at ROI-1 and ROI-2 → corresponding to the Ar plasma
- Aluminum K peak at ROI-4 → corresponds to the Al plasma electrode
- ROI-3 shows the characteristics of both groups (ROI-1-2, and ROI-4) → axial inspection
- ROI-5 shows K peaks of Fe/Co/Mn and Ni → lateral wall of the SS plasma chamber

Spectral information in ROIs

Superposition of the photon counted frames

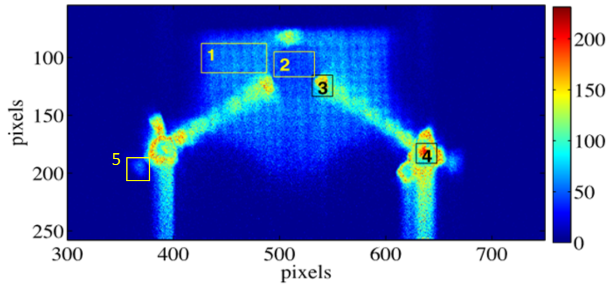

Spectral comparison at different ROIs

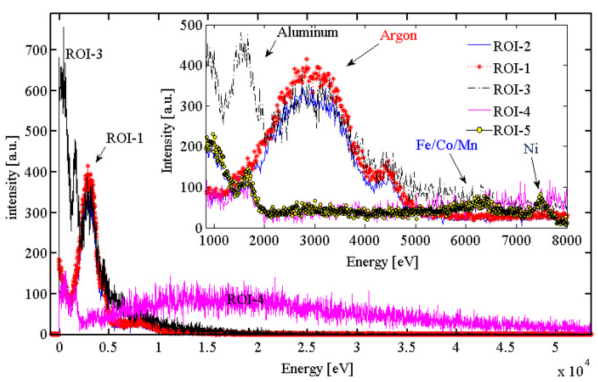

Spectra of the selected ROIs

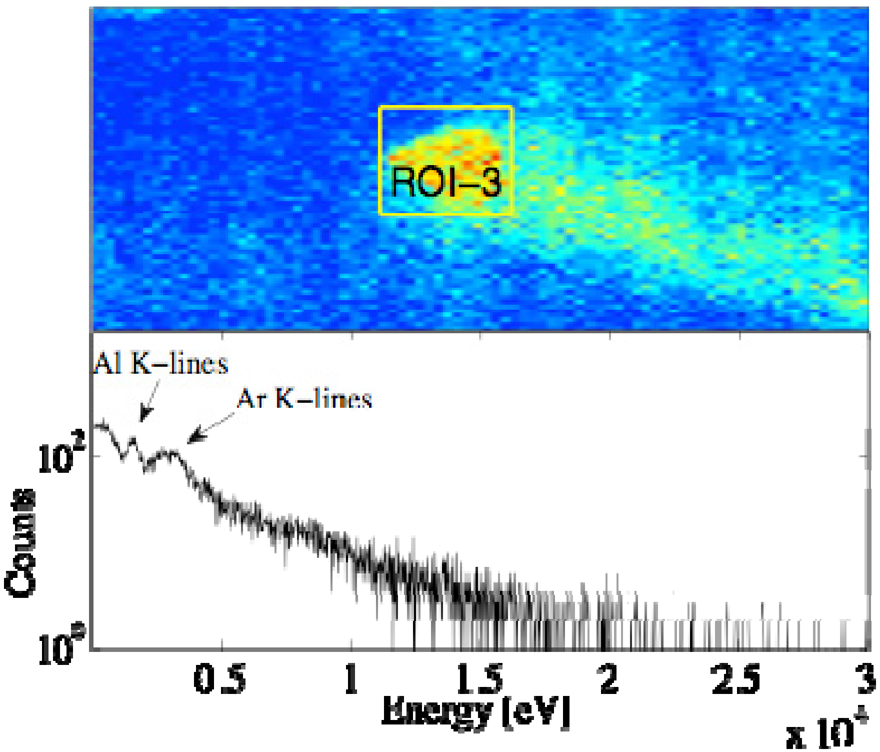

- Intense Argon K peak at ROI-1 and ROI-2 → corresponding to the Ar plasma
- Aluminum K peak at ROI-4 → corresponds to the Al plasma electrode
- ROI-3 shows the characteristics of both groups (ROI-1-2, and ROI-4) → axial inspection
- ROI-5 shows K peaks of Fe/Co/Mn and Ni → lateral wall of the SS plasma chamber

Spectral information in ROIs

Superposition of the photon counted frames

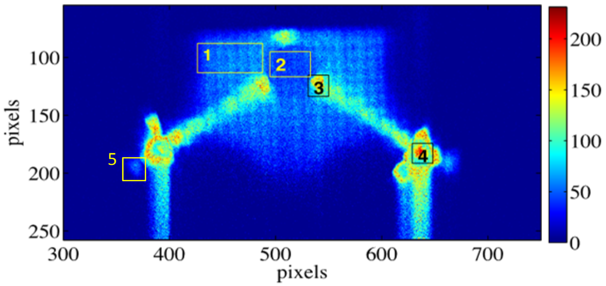

Spectral comparison at different ROIs

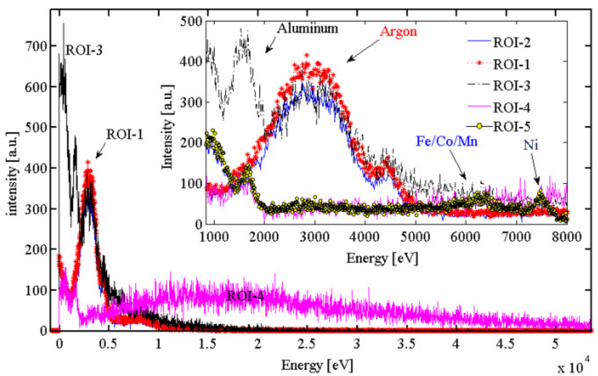

Spectra of the selected ROIs

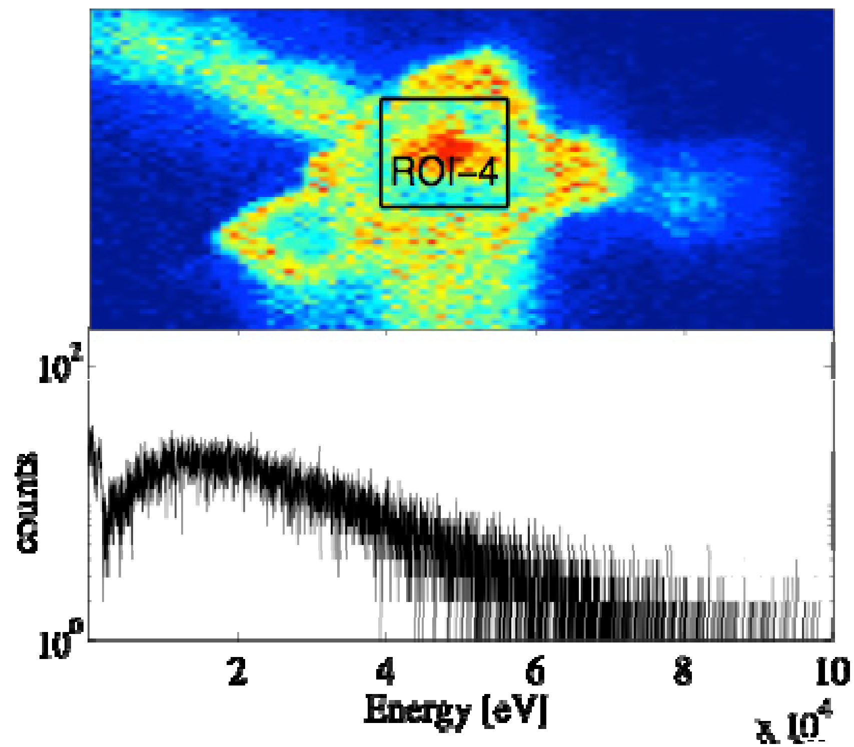

- Intense Argon K peak at ROI-1 and ROI-2 → corresponding to the Ar plasma
- Aluminum K peak at ROI-4 → corresponds to the Al plasma electrode
- ROI-3 shows the characteristics of both groups (ROI-1-2, and ROI-4) → axial inspection
- ROI-5 shows K peaks of Fe/Co/Mn and Ni → lateral wall of the SS plasma chamber

Spectral information in ROIs

Superposition of the photon counted frames

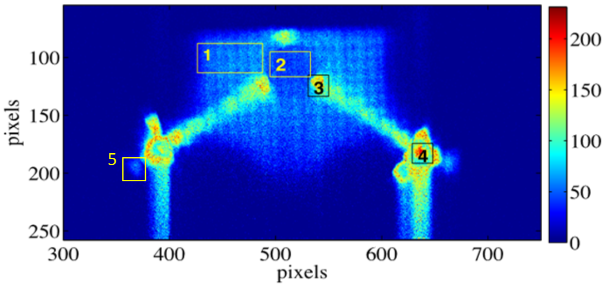

Spectral comparison at different ROIs

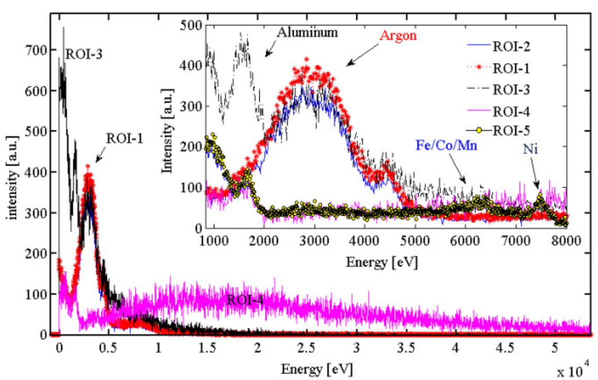

Spectra of the selected ROIs

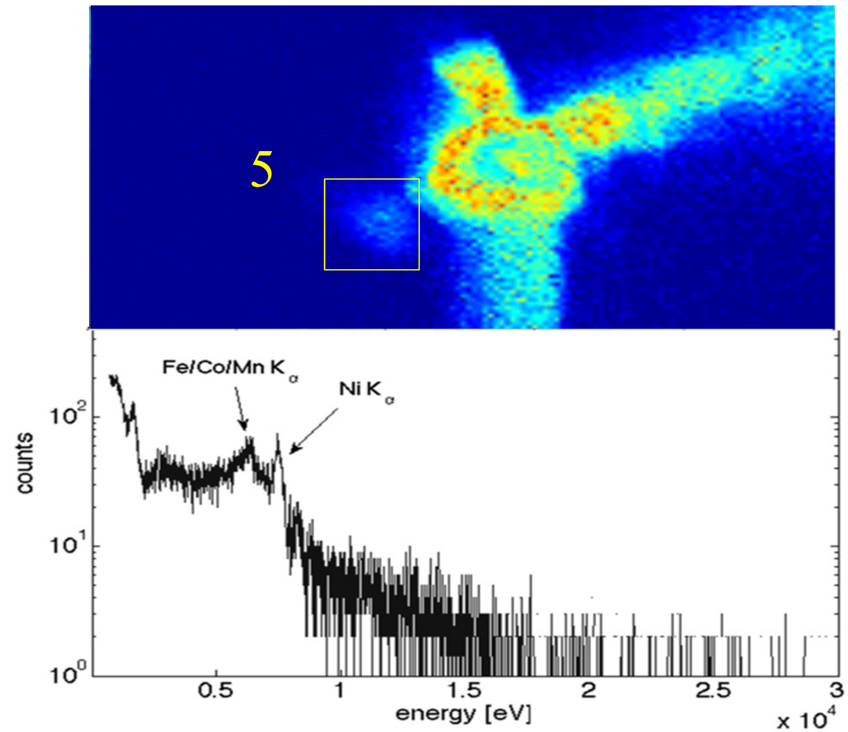

- Intense Argon K peak at ROI-1 and ROI-2 → corresponding to the Ar plasma
- Aluminum K peak at ROI-4 → corresponds to the Al plasma electrode
- ROI-3 shows the characteristics of both groups (ROI-1-2, and ROI-4) → axial inspection
- ROI-5 shows K peaks of Fe/Co/Mn and Ni → lateral wall of the SS plasma chamber

Energy filtering

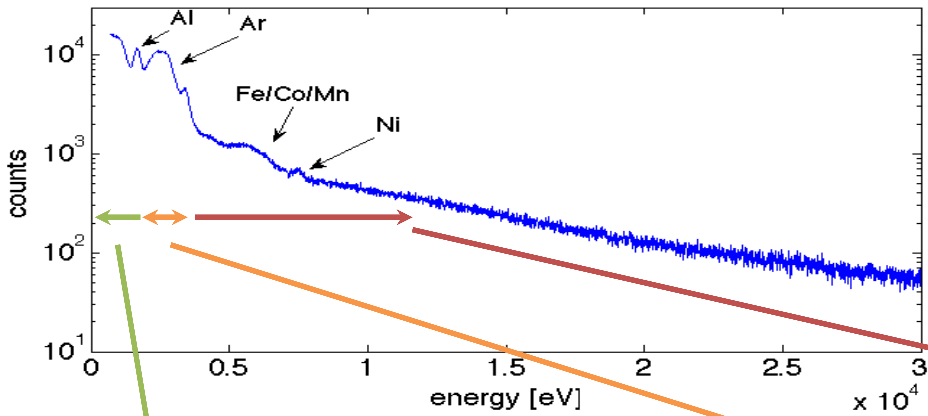

Selecting only the pixels of the frames which are loaded by the photons having energy correspond to:

- ‚Low' energy E < 2 keV
- Argon K-alpha line 2 keV < E < 4 keV
- ‚High' energy E > 4 keV

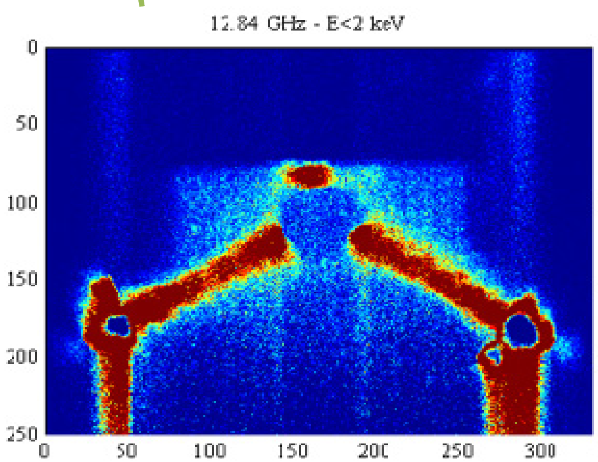

Low energy electrons lose mainly axially

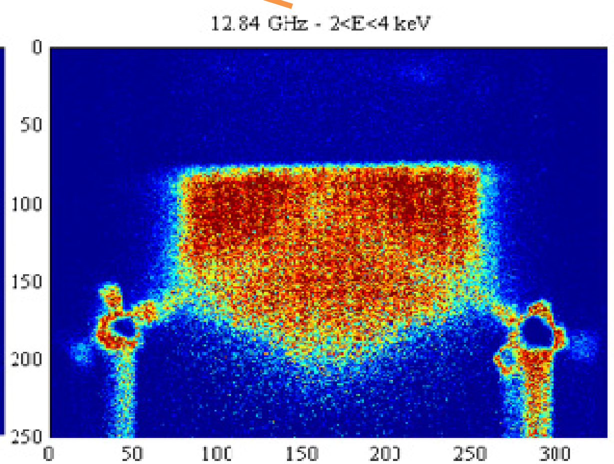

Spatial distribution of the argon plasma; dense in magnetic gap position

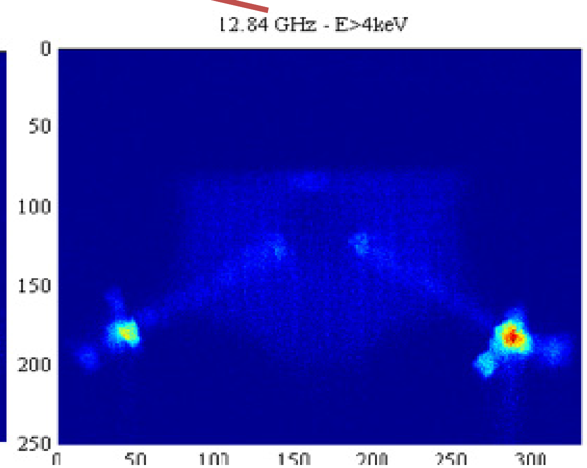

High energy electrons lose mainly radially

Plasma distribution vs frequency

Selection of the frequencies for photon counting imaging

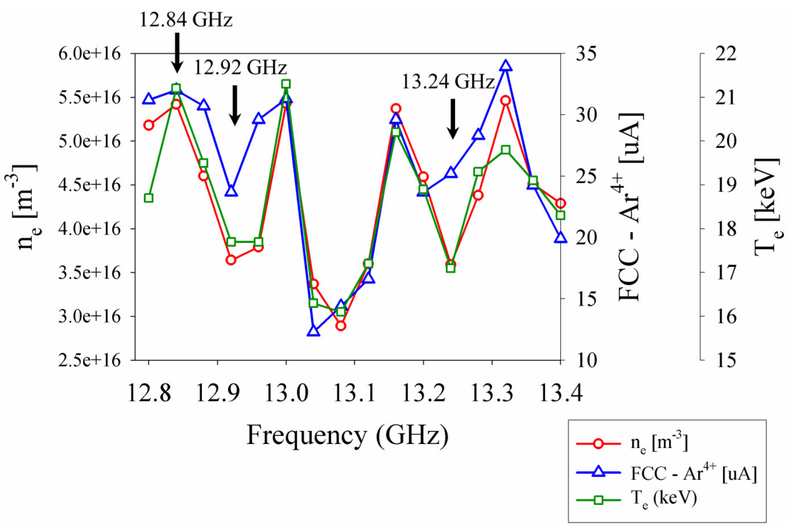

- Plasma distribution at near axis region depends on the rf frequency
- High density and high <Q> correspond to smooth distribution profile

Effect of the frequency

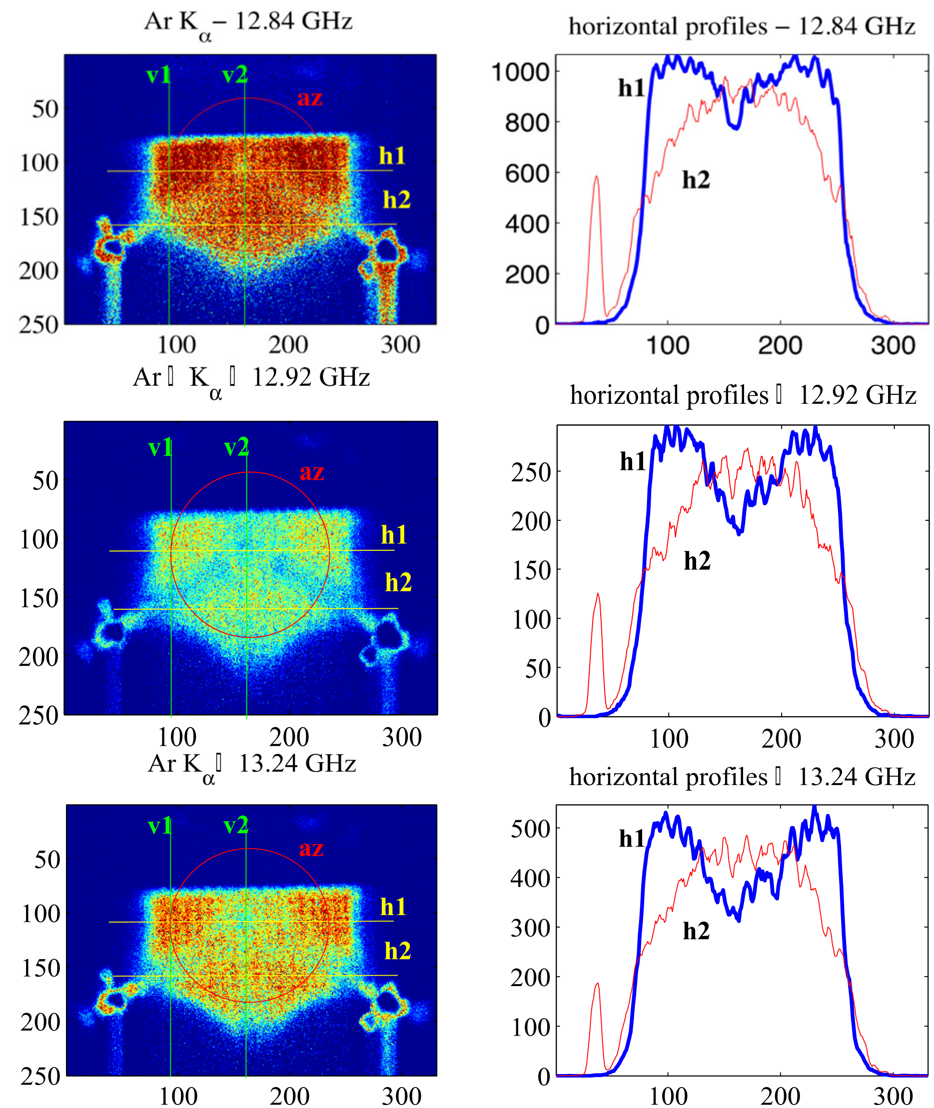

R. Rácz, ECRIS16, Busan, Korea, 29 August 2016

Perspectives

- More detailed analysis of the (integrated and PhC) images
- Comparison with modelling
- Investigation of 2f heated plasmas
- Finding correlation between beam profile and plasma shape
- Using the obtained information for mw absorption oriented design